Preliminary Design of a Distributed Facesheet Acoustic Liner for Broadband Acoustic Attenuation

Martha C. Brown*, Douglas M. Nark†, and Michael G. Jones‡
NASA Langley Research Center, Hampton, VA 23681

2023 AIAA AVIATION Forum
12-16 June 2023; San Diego, CA

The purpose of this study is to investigate the acoustic performance of a liner with a distributed facesheet and a uniform depth core for broadband attenuation. The distributed facesheet is comprised of a cluster of three distinct cell resonators of varying hole diameter and porosity replicated over the active liner treatment area. A target frequency range of 1000 to 2000 Hz and an attenuation metric of 10 dB are chosen. An optimizer is used to determine the optimal facesheet designs for flow conditions of Mach 0.0 and Mach 0.3. The samples were tested in the Grazing Flow Impedance Tube at the NASA Langley Research Center. The two liners achieved at least 10 dB attenuation over frequency ranges of 700 and 400 Hz, respectively, when tested at their respective designed flow speeds of Mach 0.0 and 0.3. This study demonstrates that a distributed facesheet with a uniform depth core can be successfully used to achieve broadband sound absorption.

I. Introduction

In communities close to airports, aircraft noise can be harmful to public health. As a result, many airports restrict operations (i.e., takeoffs and landings) to lessen the noise they generate in these communities.[1] These limitations hinder the aviation industry, a significant economic engine for the United States, from growing. The creation of new technologies that can lessen airplane noise is, therefore, of great interest to the aviation industry. The acoustic liner is one technology that is frequently used to reduce noise from the engines, and more specifically from ducted turbofans. Traditional liners are resonant absorbers that are excellent for tonal noise and are often fitted in the walls of the engine nacelles. New variable impedance liners are being designed to reduce broadband as well as tonal noise because modern high bypass ratio engines also have a significant broadband component. Manufacturers want access to adaptable, precise, and effective modeling tools that can accurately predict the impact of the acoustic liners on radiated noise in order to facilitate the development of these new liners and ultimately reduce airplane noise.

Engine nacelles typically use conventional single-layer acoustic liners, which have a perforated facesheet over a honeycomb core, to lessen fan noise. However, broadband acoustic liner designs have drawn more attention in recent years. One promising broadband design that consists of groups of resonators tuned to different frequencies is called a distributed facesheet liner. In this study, tuning is done by varying the porosity and hole diameter for the portion of the facesheet that covers each resonator. This configuration can be easily achieved using additive manufacturing or by employing robotics with more conventional manufacturing approaches. When groups of resonators with distinct facesheet configurations are combined into unit cells and then repeated over the entire surface of the liner, this type of liner can be simulated using a uniform smeared impedance (or effective impedance), where the attenuation bandwidth can be increased from tonal toward broadband.

*Senior Research Engineer, Research Directorate, Aeroacoustics Branch, martha.c.brown@nasa.gov.
†Senior Research Scientist, Research Directorate, Structural Acoustics Branch, AIAA Associate Fellow.
‡Senior Research Scientist, Research Directorate, Structural Acoustics Branch, AIAA Associate Fellow.

The concept of a distributed facesheet liner was inspired by the variable depth liner concept developed by researchers at the NASA Langley Research Center. Jones et al.[2] investigated variable depth liners with and without grazing flow for broadband noise reduction. Schiller and Jones[3] developed a semianalytical impedance model for variable depth liners. Galles et al.[4] implemented an optimization methodology to tune a liner with variable core depth.

This investigation is a continuation of a previous study evaluating the acoustic benefits of a distributed facesheet liner for broadband noise reduction.[5,6] The objective of this study is to optimize the facesheet geometries based on a range of target frequencies and flow conditions. A target frequency range of 1000 to 2000 Hz is selected for three-cell resonators, with a target attenuation of 10 dB. An optimization methodology is used to determine the best facesheet designs for a 2" by 17.6" Grazing Flow Impedance Tube (GFIT) configuration, optimized at Mach 0.0 and 0.3. Those designs are fabricated and tested. Results show that a distributed facesheet liner optimized for Mach 0.0 can attenuate at least 10 dB over a 700 Hz frequency range. Similarly, a distributed facesheet liner optimized for Mach 0.3 can attenuate at least 10 dB over a 400 Hz frequency range.

The paper is organized as follows: Section II describes the acoustic liner design methodology; Section III presents the two distributed facesheets fabricated and tested in the GFIT; Section IV discusses the acoustic performance of these distributed facesheets and Section V reviews the highlights of the paper and potential follow-on research opportunities.

II. Acoustic Liner Design

The acoustic liner design methodology used in this investigation was developed by members of the NASA Langley Liner Physics Team, and details for different research applications are described in previous papers.[4,7–9] In those investigations, optimization tools were used to control the characteristics of the core for broadband applications. In this investigation, the focus is on optimizing the facesheet parameters to produce a broadband liner with a constant-depth core. An acoustic duct propagation code is used to predict optimum impedance spectra over a number of frequencies and flow conditions. Acoustic liner modeling methods are then utilized to find geometric liner parameters (within manufacturing restrictions) required to achieve impedance spectra that best match the projected optimum values. The calculated impedance values are then used within the propagation code to predict attenuation spectra. Iteration between the prediction and design stages allows refinement of the liner design (e.g., to account for manufacturing constraints).

A. Computational Domain

For a particular application, a computational domain must be defined to model the aeroacoustic domain of a test section. In this case, the aeroacoustic domain is the NASA Langley Grazing Flow Impedance Tube (GFIT) test section. Details of the test rig will be discussed in Section III.B, but a schematic diagram of the test section is shown in Fig. 1. The leading and trailing edges of the liner (designated by L_1 and L_2) are located at $x = 8.25$" and $x = 25.85$", respectively. Thus, the length of the active liner is 17.60". The axial length of the aeroacoustic domain is $L = 40$".

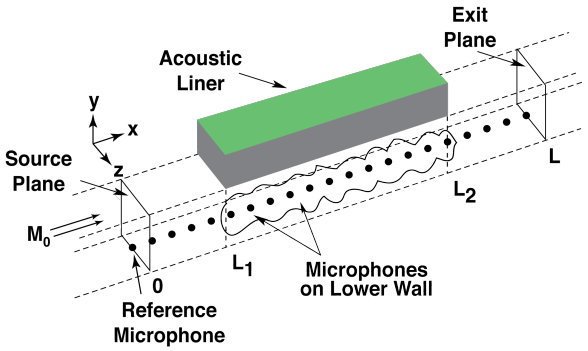

Figure 1: Schematic diagram of Grazing Flow Impedance Tube (GFIT) test section.

B. Acoustic Propagation Code

The Convected Helmholtz Equation code (CHE)[10] is the duct acoustic propagation code used for this investigation. This code is described in detail in the cited literature; therefore, only those details pertinent to this investigation are discussed. The CHE code solves the convected Helmholtz equation using a uniform flow profile. It assumes that the liner is installed on the upper wall (as in the GFIT) and permits the impedance to vary along the axial length of the liner. The CHE propagation code was used to determine the target impedance values, $\zeta_{opt}(f_i)$, at select frequencies, f_i, for a given flow speed over a design space encompassing resistance (real component of $\zeta_{opt}(f_i)$) values of $0 < \theta \leq 5$ and reactance (imaginary component of $\zeta_{opt}(f_i)$) values of $-10 < \chi \leq 10$. Optimal impedance values were determined by combining the CHE code with optimization tools available in the SciPy[11] library optimization package.

Figure 2 shows the optimum impedances of a GFIT configuration for Mach 0.0 and Mach 0.3. In this process, the liner facesheet parameters are optimized to best match the target impedances at selected target frequencies. The optimum impedances are normalized by ρc, where ρ is the density of air, and c is the speed of sound of air.

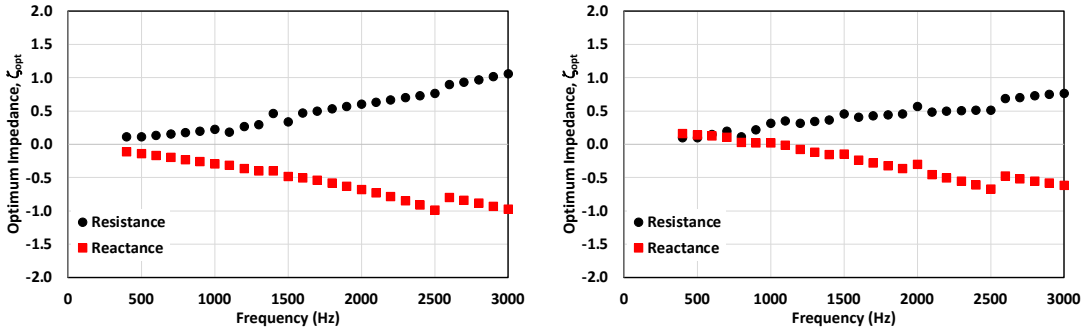

(a) Optimum impedance at Mach 0.

(b) Optimum impedance at Mach 0.3.

Figure 2: Normalized optimum impedances for GFIT configuration.

C. Semianalytical Impedance Model

For the distributed facesheet concept considered in this investigation, a broadband sound absorption is achieved as a result of the variable impedance produced by the combination of facesheet geometric parameters. Manufacturing constraints must also be included within the design process.

Figure 3 shows a side view of a liner comprised of three distinct chambers with different impedances (i.e., noted as $\zeta_{fs,i}$). Each chamber has a unique open area ratio, σ, and hole diameter, d, with a fixed facesheet thickness, t, and core depth, h. The boundary between the cell and the facesheet is represented by a dotted green line and the facesheet is represented in blue. The surface of the facesheet is represented by a red dash-dotted line. The active surface of each cell is bounded by a vertical dashed line.

The semianalytical impedance model contains two parts: the Zwikker-Kosten Transmission Line (ZKTL) model[12] and the Motsinger-Kraft facesheet model.[13] The ZKTL model uses a transmission line formulation to calculate the acoustic pressure, p_i, acoustic particle velocity, v_i, and acoustic impedance, ξ_i, at the surface of the liner cell. The facesheet model is a lumped parameter model used to predict the change in impedance across the facesheet thickness.

Starting at the hardwall backplate, the normalized acoustic pressure is set to $p_0 = 1$ and the normalized acoustic velocity, $v_0 = 0$. The ZKTL model is used to calculate the normalized acoustic pressure, p_1, and acoustic velocity, v_1, at the facesheet lower boundary, from which the normalized acoustic impedance, ξ_1, is calculated. The normalized impedance is used as input into the facesheet lumped parameter model to

predict the surface impedance, $\zeta_{fs,1}$. For multiple, unique chambers with their own respective impedances, the distributed impedance, smeared across the liner surface, ζ_s, is given by

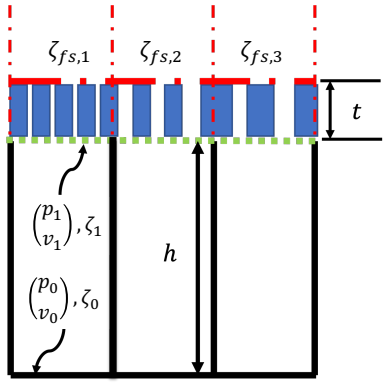

Figure 3: A distributed facesheet liner with three different cells, comprising their respective open area ratio, σ, and hole diameter, d, with a fixed facesheet thickness, t, and core depth, h.

$$\zeta_s = \left[\sum_{i=1}^{N_c} \left(\Omega_i \beta_{fs,i} \right) \right]^{-1}, \tag{1}$$

where Ω_i is the surface open area ratio, $\beta_{fs,i}$ is the surface admittance (i.e., inverse of impedance) of the ith chamber, and N_c is the total number of chambers, ($N_c = 3$ in this investigation).

D. Optimization Method

A gradient descent optimizer[11] was used to design the distributed facesheet liners in this study. By carefully selecting the objective function (i.e., optimum impedance defined over a range of frequencies as discussed in Section II.B), the objective is to determine the facesheet parameters: open area ratio, σ, and hole diameter, d, that produce impedance spectra that most closely match the target values (note that thickness, t, is fixed in the simulation). For each simulation, a combination of three target frequencies ranging from 1000 to 2000 Hz was selected. Table 1 outlines system properties for an acoustic liner, identifying the minimum and maximum bounds for each property, as well as any fixed values. The ranges were chosen to be representative of current manufacturing processes.

Table 1: Liner properties for optimizer.

Property	Value
cell depth, h	1.51”
Facesheet thickness, t	0.030” and 0.060”
Facesheet Open Area Ratio, σ	0.040 to 0.160
Facesheet Hole Diameter, d	0.020” to 0.090”
Frequency Range	1000 to 2000 Hz

The optimizer attempts to minimize the objective function, F, to find open area ratio/hole diameter combinations that meet the optimum impedance at a specified target frequency to within an acceptable tolerance. The objective function, F, is defined by Nark and Jones[14] as:

$$F = \left\{ \sum_{i=1}^{N_f} W_i \left[\zeta_{opt}\left(f_i\right) - \zeta_{pred}\left(f_i\right) \right] \left[\zeta_{opt}\left(f_i\right) - \zeta_{pred}\left(f_i\right) \right]^* \right\}^{0.5} \tag{2}$$

where i is the specific target frequency, N_f is the total number of target frequencies, $\zeta_{opt}\left(f_i\right)$ is the optimum impedance at a specific target frequency, f_i, and the predicted impedance computed from the semianalytical impedance model is $\zeta_{pred}\left(f_i\right)$. The asterisk, *, denotes the complex conjugate. For the GFIT, the optimum impedance is shown in Fig. 2. In this investigation, all frequencies were equally weighted ($W = 1$). In the beginning of the optimization study, both the resistance and reactance components of impedance were included in the objective function. However, the optimizer was unable to converge on a solution based on this objective function. The authors then decided to target reactance only (highlighted in red in Fig. 2) as the target resistance values were low and difficult to achieve (particularly in the presence of flow). Metrics of "success" were defined as the combination of frequencies over which the attenuation remained over 10 dB. These metrics helped guide the best selection to build and test.

Figure 4 shows a representative attenuation plot based on simulations for distributed facesheet liners at target flow conditions of Mach 0.0 and 0.3. The source sound pressure level (SPL) was set to 120 dB, and the facesheet thickness was held constant at 0.060". The 10 dB attenuation metric is annotated in the figure for the reader's reference. Figure 4a shows results for the facesheet optimized for the Mach 0.0 condition. Two target frequencies are held fixed (in this example, 1000 and 1200 Hz) and the third target frequency is successively set to 1400, 1600, and 1800 Hz. Note that when the target frequencies are close together, there is one peak; as the target frequencies move apart, the bandwidth gets wider and multiple attenuation peaks are present. There is a similar behavior for the facesheet optimized for Mach 0.3 in Fig. 4b. These plots served as a guide in selecting the combination of target frequencies that gives the widest bandwidth of attenuation over 10 dB. For a liner optimized for Mach 0.0, 120 dB, target frequencies of 1000, 1200, and 1600 Hz were selected for fabrication. For a liner optimized for Mach 0.3, 120 dB, target frequencies of 1000, 1300, and 1600 Hz were selected for fabrication. Each three-cell combination had different hole diameter and porosity combinations that were fabricated and tested in the GFIT. For the 1000-1200-1600 Hz combination of target frequencies selected in Fig. 4a, the bandwidth satisfying the attenuation criterion is about 650 Hz. For the 1000-1300-1600 Hz combination of target frequencies in Fig. 4b, the bandwidth satisfying the attenuation criterion is about 400 Hz. The reader should note that the broadband attenuation range decreased when optimized for flow.

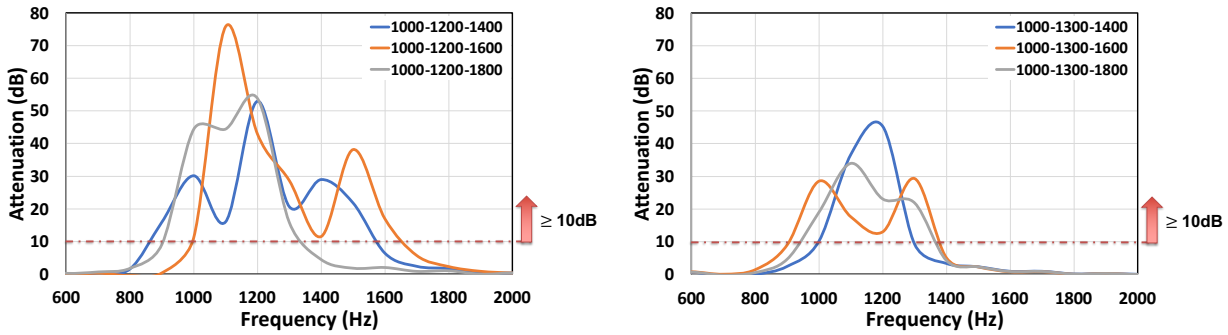

(a) Optimized for Mach 0.

(b) Optimized for Mach 0.3.

Figure 4: Predicted attenuation spectra from distributed facesheet liners at target flow conditions Mach 0.0 and 0.3, and source SPL of 120 dB for a facesheet thickness of 0.060".

III. Experimental Method

A. Evaluation Liners

Two evaluation liners optimized for Mach 0 and 0.3 flow conditions were fabricated and tested. Table 2 describes the three-cell characteristics of these liners. Each liner used in this study consists of a nonuniform perforate facesheet, rectangular core chambers, and a rigid backplate. The two facesheet samples were fabricated with a fixed facesheet thickness, $t = 0.060$". Both samples used the same core depth, $h = 1.51$", and had an active liner length of 17.60". The active liner length is the total axial length of acoustic treatment. To account for the partition thickness (shoulders) in the smeared impedance calculation, the leading edge of the active liner is assumed to start at one-half a partition thickness upstream of the first cell. Similarly, the trailing edge of the active liner length ends at one-half a partition thickness downstream from the last cell. The partition thickness (shoulders) are accounted for in the smeared impedance. Each distributed facesheet was 3D printed via stereolithography (SLA). Figures 5 and 6 show the facesheet sample optimized for flow conditions Mach 0 and 0.3, respectively. The reader should note that in the close-up views of both facesheets (Figs. 5b and 6b), the three-cell pattern repeats over the active liner area of 2" x 17.60".

Table 2: GFIT three-cell characteristics for distributed porosity and hole diameter facesheets.

Optimization	Cell 1	Cell 2	Cell 3
Mach 0.0	$d = 0.081", \sigma = 0.057$	$d = 0.064", \sigma = 0.108$	$d = 0.030", \sigma = 0.157$
Mach 0.3	$d = 0.030", \sigma = 0.047$	$d = 0.056", \sigma = 0.055$	$d = 0.086", \sigma = 0.128$

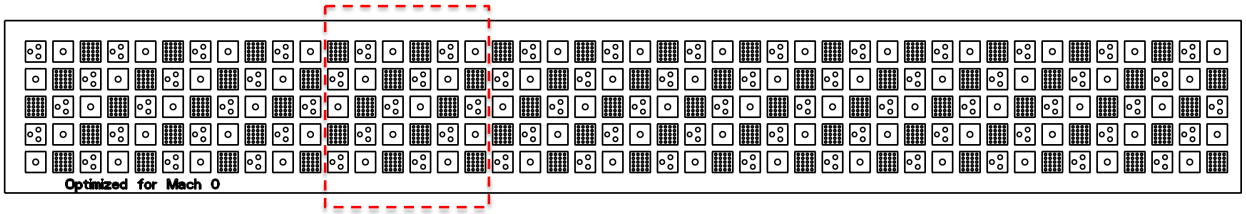

(a) Schematic diagram.

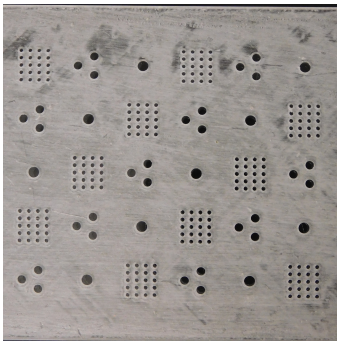

(b) Close-up picture of facesheet [Source: NASA].

Figure 5: GFIT sample optimized for no-flow condition and source SPL of 120 dB.

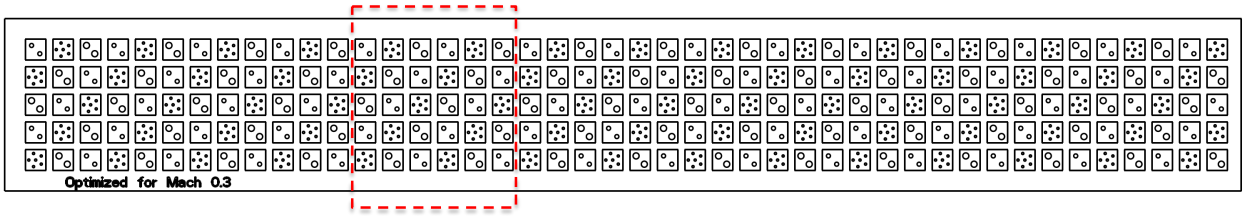

(a) Schematic diagram.

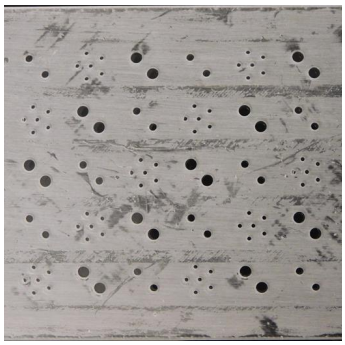

(b) Close-up picture of facesheet [Source: NASA].

Figure 6: GFIT sample optimized for Mach 0.3 and source SPL of 120 dB.

B. Grazing Flow Impedance Tube (GFIT)

The GFIT (see Fig. 7) is utilized to assess the acoustic performance of each liner. The cross-sectional geometry of the GFIT, which is 2.0" wide by 2.50" tall, is such that higher-order modes in the horizontal and vertical dimensions cut on at separate frequencies. The test section permits the evaluation of acoustic liners ranging in length from 2" to 24". The surface of the test liner forms a portion of the upper wall of the flow duct. Each sample has an overall length of 18" for this investigation, which includes the active acoustic treatment and hardwall. The source section is comprised of twelve acoustic drivers mounted upstream (exhaust mode) of the test section. The tonal source is stepped between 400 and 3000 Hz in 100 Hz increments while the source amplitude is kept constant (within 0.5 dB of the desired sound pressure level). This investigation evaluated source amplitude levels of 120 and 140 dB. In this diagram, the GFIT is configured to operate in aft mode, where the sound travels in the same direction as the flow. These experiments were conducted at Mach 0.0, 0.3, and 0.5.

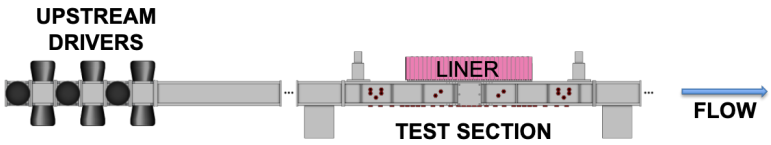

Figure 7: Artist rendition of Grazing Flow Impedance Tube (GFIT).

Fifty-three flush-mounted microphones located in the lower wall (opposite the liner) are used to measure the acoustic pressure field over the axial length of the test section, $L = 40$" (see Figure 1). A cross-spectrum signal extraction method[15] is used to determine the amplitudes and phases at each of the microphone locations relative to the amplitude and phase at the reference microphone location.

C. Impedance Eduction Method

Each liner was evaluated using a conventional impedance eduction approach.[16–18] Figures 8 and 9 show results for liners optimized for the Mach 0.0 and 0.3 flow conditions, respectively. The three curves represent impedance spectra educed with each of these liners exposed to a source SPL of 120 dB and mean flows of Mach 0.0, 0.3, and 0.5. Results at 140 dB showed a similar behavior; therefore, the results are not presented in this paper. The resistance spectra for both distributed facesheet samples (Figs. 8a and 9a) show an increase in resistance as the flow velocity is increased, as expected. The reactance spectra for both distributed facesheet samples (Figs. 8b and 9b) show a noticeable reduction in slope as the Mach number is increased.

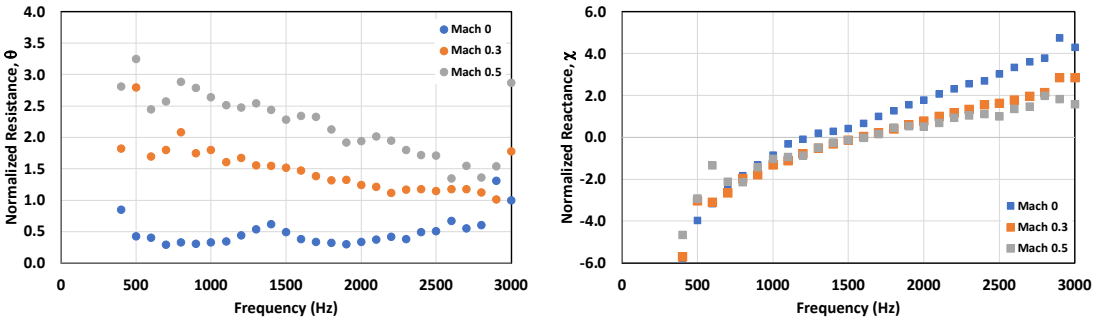

(a) Normalized Resistance.

(b) Normalized Reactance.

Figure 8: Impedance spectra for liner facesheet optimized for Mach 0.0 and source SPL of 120 dB.

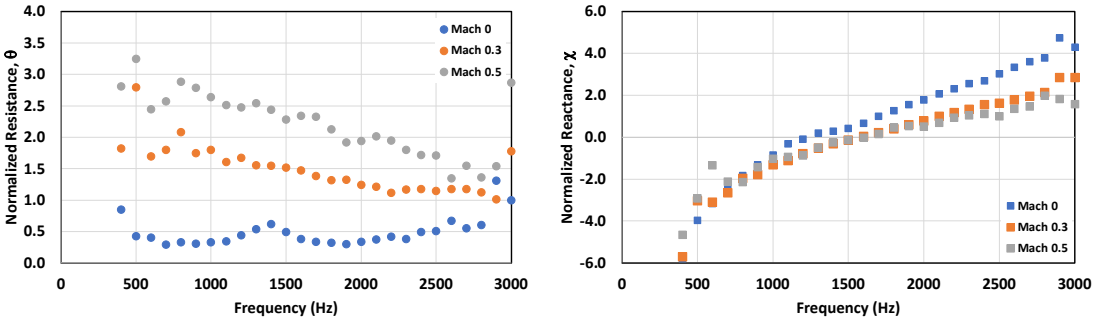

(a) Normalized Resistance.

(b) Normalized Reactance.

Figure 9: Impedance spectra for liner facesheet optimized for Mach 0.3 and source SPL 120 dB.

IV. Results and Discussion

The purpose of this investigation is to create a uniform depth broadband acoustic liner with a nonuniform perforate facesheet. The nonuniform perforate facesheet is designed by changing the hole diameter and porosity over each chamber. A three-chamber variation was selected where the facesheets were optimized for Mach 0.0 and 0.3 at 120 dB. The three-chamber variation is simulated using a uniform smeared impedance (i.e., effective impedance) tuned over a desired frequency range at a specified flow condition.

The study was divided into four stages. First, the optimum impedance spectrum for the GFIT is calculated at select flow conditions using the CHE propagation code. Optimum impedance is defined as the impedance that provides maximum attenuation. Second, liner modeling tools are coupled with an optimizer to best match target impedances from the previous step, guided by physical constraints provided by the liner designer. If the optimizer is unable to converge on a solution, then the physical constraints are updated and

predicted impedances are evaluated. In this study, the optimizer was unable to achieve acceptable attenuation by targeting resistance and reactance simultaneously. Therefore the optimizer was modified to target reactance only. Third, converged solutions are matched against the metrics defined, and top candidates are fabricated and tested. Finally, results are compared to CHE predictions to validate the liner design process.

Figures 10, 11, and 12 show the measured SPL axial profiles for Mach 0.0, 0.3, and 0.5, respectively, for the two distributed facesheet liners. Each figure displays the location of the liner with respect to the test section. The performance metric is highlighted in a red dash-dotted line at 110 dB so the reader can easily view the response of sound attenuation for each frequency. A red arrow pointing downward indicates attenuation exceeding the performance metric.

A number of interesting features are observed. When the liner optimized at Mach 0.3 is tested at Mach 0.0, the attenuation at 1200 Hz is actually larger than for the liner optimized at Mach 0.0 (see Fig. 10b). Figure 11a shows that for a liner optimized at Mach 0.0 and tested at Mach 0.3, the attenuations at 1400, 1600, and 1800 Hz are larger than for the liner optimized at Mach 0.3. For the Mach 0.5 flow condition, target metrics were not met (10 dB attenuation), as expected since the distributed facesheets were not optimized at Mach 0.5.

Figure 13 shows the measured attenuation spectra for the two distributed facesheet liners at the three flow conditions. The measured attenuation spectra were computed by subtracting the SPL level at the exit plane ($x = 40$") from the SPL at the inlet plane ($x = 0$"). The performance metric is highlighted in a red dash-dotted line at 10 dB so the reader can easily view the response of sound attenuation for each frequency. A red arrow pointing upward indicates attenuation exceeding the performance metric. For the distributed facesheet liner optimized at Mach 0.0, the frequency range for which the attenuation is at least 10 dB is approximately 700 Hz (1050-1750 Hz) when tested at Mach 0.0 (Fig. 13a). Similarly, for the distributed facesheet liner optimized at Mach 0.3, the frequency range is approximately 400 Hz (1350-1750 Hz) when tested at Mach 0.3 (Fig. 13b). It is interesting to note how well the liner optimized for Mach 0.3 performs at the Mach 0.0 flow condition. These frequency ranges for both distributed facesheet liners compare well with prediction (see Section II.D). In comparison with a uniform liner with similar geometric parameters, the frequency range for which the attenuation is at least 10 dB is approximately 350 Hz for Mach 0.0.

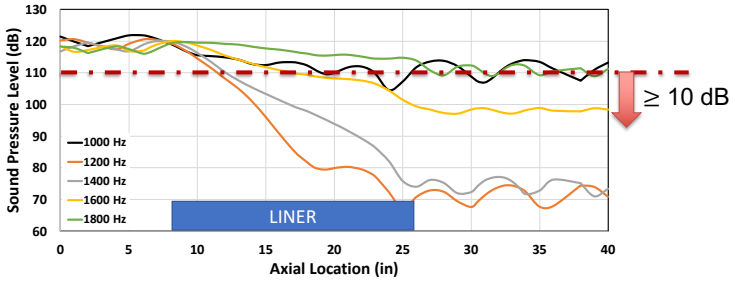

(a) SPL profiles for facesheet optimized for Mach 0.

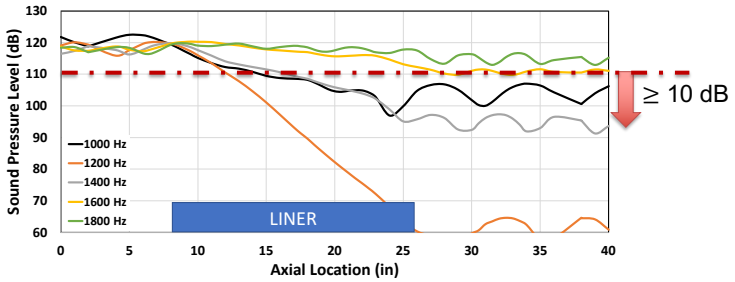

(b) SPL profiles for facesheet optimized for Mach 0.3.

Figure 10: Measured SPL axial profiles for the Mach 0.0 flow condition and source SPL of 120 dB.

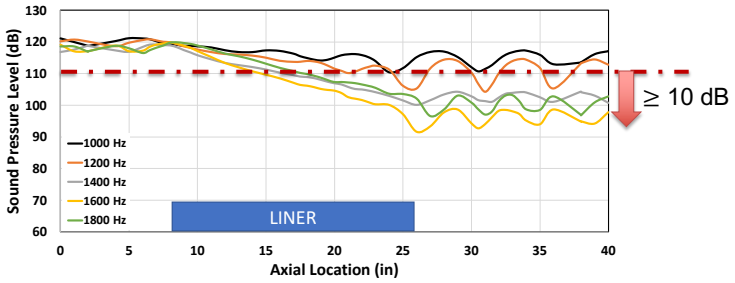

(a) SPL profiles for facesheet optimized for Mach 0.

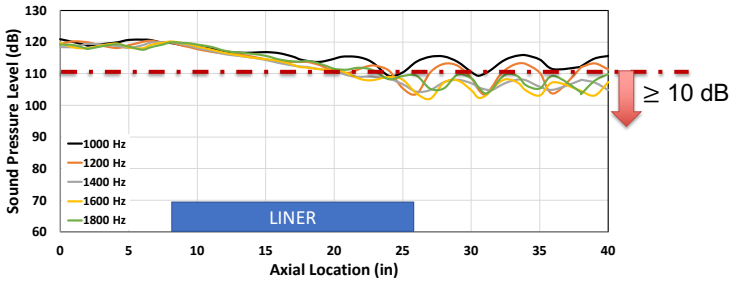

(b) SPL profiles for facesheet optimized for Mach 0.3.

Figure 11: Measured SPL axial profiles for the Mach 0.3 flow condition and source SPL of 120 dB.

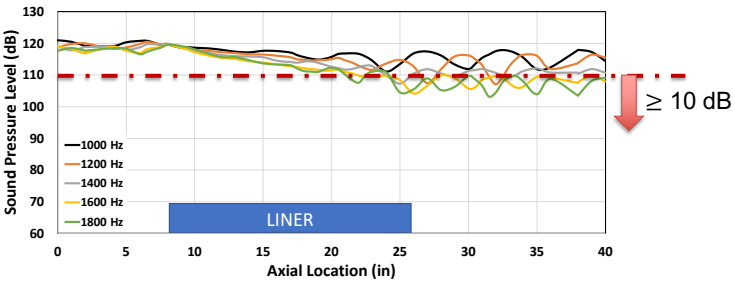

(a) SPL profiles for facesheet optimized for Mach 0.

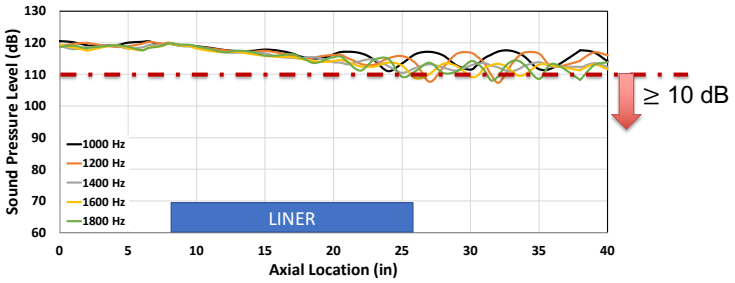

(b) SPL profiles for facesheet optimized for Mach 0.3.

Figure 12: Measured SPL axial profiles for the Mach 0.5 flow condition and source SPL of 120 dB.

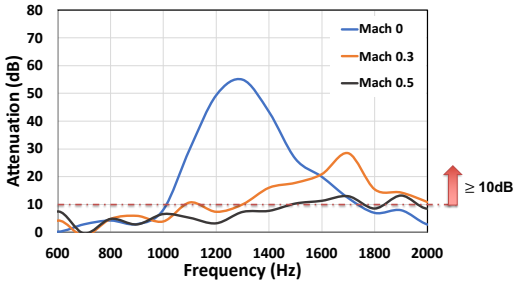

(a) Optimized for Mach 0.

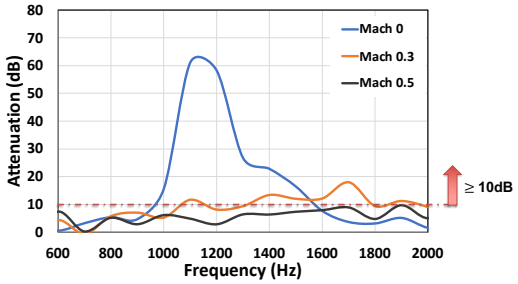

(b) Optimized for Mach 0.3.

Figure 13: Measured attenuation spectra for distributed facesheet liners optimized at Mach 0.0 and 0.3, for flow conditions of Mach 0.0, 0.3, and 0.5, and source SPL of 120 dB.

V. Concluding Remarks

The goal of this study was to explore a distributed facesheet with a uniform depth core acoustic liner for broadband attenuation. A target frequency range of 1000 to 2000 Hz was selected for three-cell resonators, with a target attenuation metric of 10 dB. An optimizer was used to determine the best facesheet designs for Mach 0.0 and 0.3 flow conditions. Results showed that a distributed facesheet liner optimized for Mach 0.0 could attenuate the sound by at least 10 dB over a frequency range of 700 Hz. This range was reduced to 400 Hz for a distributed facesheet liner optimized for Mach 0.3. This study demonstrated that broadband attenuation can be achieved with a distributed facesheet and uniform depth core. Future studies will focus on evaluating the efficacy of a distributed facesheet liner for use in more complex aeroacoustic environments. Specifically, samples targeting different frequency ranges and flow conditions will be tested in the NASA Langley Curved Duct Test Rig, where the acoustic source consists of controlled higher-order modes.

Acknowledgments

The authors would like to thank the following people who were instrumental to the success of this investigation: Mr. Alonzo (Max) Reid in the Aeroacoustics Branch for outstanding testing support, Mr. Christopher (Mark) Cagle in the Aeronautics Systems Engineering Branch for outstanding support in designing the samples, and Mr. Robert C. Andrews in the Manufacturing Applications Branch for outstanding 3D printing services. This work was funded by the Advanced Air Transport Technology Project of the NASA Advanced Air Vehicles Program.

References

[1]Smith, M. J. T., *Aircraft Noise*, Cambridge University Press, 2004.

[2]Jones, M. G., Watson, W. R., Nark, D. M., and Howerton, B. M., "Evaluation of Variable-Depth Liner Configurations for Increased Broadband Noise Reduction," AIAA Paper 2015-2697, 21st AIAA/CEAS Aeroacoustics Conference, Dallas, TX, June 2015.

[3]Schiller, N. H. and Jones, M. G., "Smeared Impedance Model for Variable Depth Liners," AIAA Paper 2018-3774, 24th AIAA/CEAS Aeroacoustics Conference, Atlanta, GA, June 2018.

[4]Galles, M. B., Jones, M. G., and Nark, D. M., "An Initial Assessment of Variable Depth Liner Optimization for Ducted Proprotor Applications," AIAA Paper 2022-2821, 28th AIAA/CEAS Aeroacoustics Conference, Southampton, UK, June 2022.

[5]Brown, M. C. and Jones, M. G., "Evaluation of Variable Facesheet Liner Configurations for Broadband Noise Reduction," AIAA Paper 2020-2616, 26th AIAA/CEAS Aeroacoustics Conference, Reno, NV, June 2020.

[6]Brown, M. C. and Jones, M. G., "Evaluation of a Variable Facesheet Liner Configuration in Grazing Incidence Flow," AIAA Paper 2021-2243, 27th AIAA/CEAS Aeroacoustics Conference, Washington, DC, June 2021.

[7]Jones, M. G., Watson, W. R., Nark, D. M., Schiller, N. H., and Born, J. C., "Optimization of Variable-Depth Liner Configurations for Increased Broadband Noise Reduction," AIAA Paper 2016-2783, 22nd AIAA/CEAS Aeroacoustics Conference, Lyon, France, May 2016.

[8]Nark, D. M., Jones, M. G., Schiller, N. H., and Sutliff, D. L., "Broadband Inlet Liner Design for the DGEN Aeropropulsion Research Turbofan," AIAA Paper 2018-3608, 24th AIAA/CEAS Aeroacoustics Conference, Atlanta, GA, June 2018.

[9]Sutliff, D. L., Nark, D. M., Jones, M. G., and Schiller, N. H., "Design and Acoustic Efficacy of a Broadband Liner for the Inlet of the DGEN Aero-propulsion Research Turbofan," AIAA Paper 2019-2582, 25th AIAA/CEAS Aeroacoustics Conference, Delft, The Netherlands, May 2019.

[10]Watson, W. R., Jones, M. G., and Parrott, T. L., "Validation of an Impedance Eduction Method in Flow," *AIAA Journal*, Vol. 37, No. 7, July 1999, pp. 818–824.

[11]Virtanen, P., Gommers, R., and Oliphant, Travis E., e. a., "SciPy 1.0: Fundamental Algorithms for Scientific Computing in Python," *Nature Methods*, Vol. 17, 2020, pp. 261–272.

[12]Zwikker, C. and Kosten, C., *Sound absorbing materials*, Elsevier Publishing Company, 1949.

[13]Motsinger, R. E. and Kraft, R. E., "Design and Performance of Duct Acoustic Treatment: Aeroacoustics of Flight Vehicles; Chapter 14, Vol. 2: Noise Control," NASA RP 1258, Aug. 1991.

[14]Nark, D. M. and Jones, M. G., "An acoustic liner design methodology based on a statistical source model," *International Journal of Aeroacoustics*, June 2021.

[15]Bendat, J. S. and Piersol, A. G., *Random Data: Analysis and Measurement Procedures*, Wiley-Interscience, 1971.

[16]de Prony, R., "Essai Éxperimental et Analytique: Sur Les Lois de la Dilatabilité de Fluides Élastique et sur Celles de la Force Expansive de la Vapeur de L'alkool, Àdifférentes Temperatures," *Journal de l'école Polytechnique*, Vol. 1, No. 22, 1795, pp. 24–76.

[17]Jones, M. G., Watson, W. R., Howerton, B. M., and Busse-Gerstengarbe, S., "A Comparative Study of Impedance Eduction Methods, Part 2: NASA Tests and Methodology," AIAA Paper 2013-2125, 19th AIAA/CEAS Aeroacoustics Conference, Berlin, Germany, May 2013.

[18]Watson, W. R., Carpenter, M. H., and Jones, M. G., "Performance of Kumaresan and Tufts Algorithm in Liner Impedance Eduction with Flow," *AIAA Journal*, Vol. 53, No. 4, April 2015, pp. 1091–1102.